Journal for ImmunoTherapy of Cancer

Combining bempegaldesleukin (CD122-preferential IL-2 pathway agonist) and NKTR-262 (TLR7/8 agonist) improves systemic antitumor CD8$^+$ T cell cytotoxicity over BEMPEG+RT

Annah S Rolig ,[1] Daniel C Rose,[1] Grace Helen McGee,[1] Werner Rubas,[2] Saul Kivimäe,[3] William L Redmond [1]

To cite: Rolig AS, Rose DC, McGee GH, *et al*. Combining bempegaldesleukin (CD122-preferential IL-2 pathway agonist) and NKTR-262 (TLR7/8 agonist) improves systemic antitumor CD8$^+$ T cell cytotoxicity over BEMPEG+RT. *Journal for ImmunoTherapy of Cancer* 2022;**10**:e004218. doi:10.1136/jitc-2021-004218

► Additional supplemental material is published online only. To view, please visit the journal online (http://dx.doi.org/10.1136/jitc-2021-004218).

Accepted 28 March 2022

[1]Earle A Chiles Research Institute, Providence Cancer Institute, Portland, OR, USA
[2]Sutro Biopharma, South San Francisco, CA, USA
[3]Nektar Therapeutics, San Francisco, CA, USA

Correspondence to
Dr William L Redmond; william.redmond@providence.org

ABSTRACT

Background Tumor cell death caused by radiation therapy (RT) triggers antitumor immunity in part because dying cells release adjuvant factors that amplify and sustain dendritic cell and T cell responses. We previously demonstrated that bempegaldesleukin (BEMPEG: NKTR-214, an immunostimulatory IL-2 cytokine prodrug) significantly enhanced the antitumor efficacy of RT through a T cell-dependent mechanism. Because RT can induce either immunogenic or tolerogenic cell death, depending on various factors (radiation dose, cell cycle phase), we hypothesized that providing a specific immunogenic adjuvant, like intratumoral therapy with a novel toll-like receptor (TLR) 7/8 agonist, NKTR-262, would improve systemic tumor-specific responses through the activation of local innate immunity. Therefore, we evaluated whether intratumoral NKTR-262 combined with systemic BEMPEG treatment would elicit improved tumor-specific immunity and survival compared with RT combined with BEMPEG.

Methods Tumor-bearing mice (CT26; EMT6) received BEMPEG (0.8 mg/kg; intravenously), RT (12 Gy × 1), and/or intratumoral NKTR-262 (0.5 mg/kg). Flow cytometry was used to evaluate CD4$^+$ and CD8$^+$ T cell responses in the blood and tumor 7 days post-treatment. The contribution of specific immune subsets was determined by depletion of CD4$^+$, CD8$^+$, or NK cells. CD8$^+$ T cell cytolytic activity was determined by an in vitro CTL assay. Data are representative of 1–2 independent experiments (n=5–14/group) and statistical significance was determined by 1-way analysis of variance (ANOVA) or repeated measures ANOVA (p value cut-off of 0.05).

Results BEMPEG+NKTR-262 significantly improved survival compared with BEMPEG+RT in a CD8$^+$ T cell-dependent manner. Response to BEMPEG+NKTR-262 was characterized by a significant expansion of activated CD8$^+$ T cells (GzmA$^+$; Ki-67$^+$; ICOS$^+$; PD-1$^+$) in the blood, which correlated with reduced tumor size ($p<0.05$). In the tumor, BEMPEG+NKTR-262 induced higher frequencies of GzmA$^+$ CD8$^+$ T cells exhibiting reduced expression of suppressive molecules (PD-1$^+$), compared with BEMPEG+RT ($p<0.05$). Further, BEMPEG+NKTR-262 treatment induced greater tumor-specific CD8$^+$ T cell cytolytic function than BEMPEG+RT.

Conclusions BEMPEG+NKTR-262 therapy elicited more robust expansion of activated CD8$^+$ T cells compared with BEMPEG+RT, suggesting that intratumoral TLR stimulation provides superior antigen presentation and costimulatory activity compared with RT. A clinical trial of BEMPEG+NKTR-262 for patients with metastatic solid tumors is in progress (NCT03435640).

Key messages

What is already known on this topic

► Combining systemic and local therapies can induce highly effective antitumor immunity. For example, combining systemic IL-2 therapy with local radiation therapy (RT) improved responses over IL-2 alone, but produced limited abscopal effects. Here, we sought to evaluate the extent to which combining BEMPEG (immunostimulatory IL-2 cytokine prodrug) with intratumoral toll-like receptor 7/8 agonist (NKTR-262) therapy would augment tumor-specific responses and increase survival as compared with BEMPEG+RT.

How this study might affect research, practice or policy

► BEMPEG+NKTR-262 induced superior systemic adaptive immunity and survival as compared with BEMPEG+RT. These data demonstrate the potent therapeutic potential of BEMPEG+NKTR-262 and suggest that clinical evaluation of this combination is warranted.

INTRODUCTION

While applications of immunotherapies, either individually or in combination with other treatments, continue to improve patient outcomes,[1 2] determining which immunotherapy combinations achieve the best possible outcome is a critical and unresolved issue. Identifying highly efficacious combination therapies will require elucidating the

molecular mechanisms by which they induce antitumor responses and an in-depth, side-by-side characterization of different therapies. Here, we compare efficacy of two combination therapies, bempegaldesleukin (BEMPEG, immunostimulatory IL-2 cytokine prodrug)[3–5] combined either with radiation therapy (RT) or with NKTR-262, a toll-like receptor (TLR) 7/8 agonist.

Cytokine-based immunotherapies aim to increase the proliferation and survival of pre-existing antitumor effector T cells. For example, high-dose IL-2 (HD IL-2) is an FDA-approved cytokine therapy with a 15%–20% objective response rate in metastatic renal cell carcinoma and melanoma.[6–8] However, HD IL-2 efficacy is limited by the expansion of suppressive $CD25^+$ $FoxP3^+$ T regulatory (Treg) cells[9] and by treatment toxicity, which includes vascular leak syndrome, hypotension, and liver toxicities.[10] One prodrug modified to reduce those toxicities is BEMPEG, an engineered IL-2R agonist with six releasable polyethylene glycol (PEG) units attached to the IL-2Rα binding region. These PEG units increase the duration of IL-2 receptor agonism and preferentially reduce binding to IL-2Rα (CD25)[5] compared with IL-2Rβ, supporting effector T cell expansion over Treg expansion, and thereby increasing efficacy and reducing toxicity. Indeed, BEMPEG-induced T cell activation and expansion activity in vivo increases Teff:Treg ratios in tumor tissue compared with IL-2.[4]

Because BEMPEG supports adaptive immunity, we sought to evaluate BEMPEG in combination with different innate immune agonists capable of boosting antitumor immunity, aiming to enhance overall therapeutic potential. Both RT and TLR targeting have innate immunostimulatory effects that can unleash antitumor $CD8^+$ T cell responses.[11 12] RT-induced tumor cell death results in increased cross-presentation of tumor antigen,[13] increased numbers of IFN-γ-secreting tumor-specific tumor-infiltrating lymphocytes (TIL),[14] and increased expression of chemokines that promote T and NK cell trafficking to the tumor.[15 16] TLR7/8 stimulation can induce functional APC differentiation,[17] induce Th1-biased responses,[18] and enhance $CD8^+$ T cell effector functions.[11] Furthermore, TLR7/8 agonists have demonstrated antitumor activity in preclinical models.[19] BEMPEG synergizes with RT and provides the greatest benefit to immunologically 'hot' (well infiltrated) tumors,[16] but only a modest benefit to immunologically 'cold' (poorly infiltrated) tumors.[20] The modest benefit observed may be a result of the immunosuppressive effects elicited by RT, which include inactivating NK cells, recruiting myeloid-derived suppressor cells (MDSCs), and altering macrophage polarization towards an M2 tumor-promoting phenotype.[21]

Whether the innate stimulation provided by the TLR7/8 agonist NKTR-262 combined with BEMPEG will improve response rates over BEMPEG +RT is unknown. We hypothesized that the proinflammatory signals provided via intratumoral NKTR-262 would enhance the priming of tumor-reactive T cells that would then be supported by systemic BEMPEG treatment, resulting in BEMPEG +NKTR-262 eliciting more robust tumor regression than BEMPEG +RT. To address these hypotheses, we comprehensively characterized functional and phenotypic immune responses induced by these two combination therapies, which provided insight into the mechanisms associated with efficacious combination therapies.

MATERIALS AND METHODS

Mice

Wild-type 6–8 week-old C57BL/6 and BALB/c mice (Jackson Labs; Bar Harbor, ME), and Nur77-GFP transgenic mice (Dr. Andrew Weinberg; EACRI, Portland, OR)[22] were bred in the EACRI facility. Mice were maintained under specific pathogen-free conditions in the Providence Portland Medical Center animal facility.

Tumor cell lines

CT26 (colon carcinoma, BALB/c), EMT6 (mammary carcinoma, BALB/c), and MCA-205 (fibrosarcoma, C57BL/6) tumor cell lines (all from ATCC) were maintained in complete RPMI-1640 (cRPMI; 10% FBS, 10 mmol/L HEPES, 1% non-essential amino acids, sodium pyruvate (Lonza), and penicillin–streptomycin–glutamine (Invitrogen)). Cell line identity was verified through monthly assessment of morphology and growth kinetics. Cell lines were tested annually using the MycoAlert mycoplasma detection kit (Lonza, Basel, Switzerland).

In vivo tumor studies

Mice were inoculated with 1×10^6 (CT26 and MCA-205) and 1×10^5 (EMT6) tumor cells in dual-flank subcutaneous injections. Tumor growth was monitored using two-dimensional (length × width) caliper measurements 2–3 ×/week. Treatments began 10 days following implant, when tumors reached 50–80 mm^2. Mice received control (diluent; 10 mM citric acid, 7% trehalose, pH 4, iv or HBSS it), RT (12 Gy), BEMPEG (Nektar Therapeutics, San Francisco, CA) (0.8 mg/kg, intravenously), NKTR-262 (Nektar Therapeutics, San Francisco, CA) (10 mg/kg, it), BEMPEG +RT, or BEMPEG +NKTR-262 concurrently. CT-guided photon RT with a beam energy of 220 kV was delivered using a Small Animal Radiation Research Platform (XStrahl, Gulmay Medical, Suwanee, GA) to an isocenter in the center of the tumor. Dosimetry was performed using Murislice software (XStrahl), and irradiated lesions received 12 Gy in a single fraction using opposed tangential fields. For survival experiments, tumor size was monitored until all animals reached a primary endpoint (tumor-free or total tumor burden >250 mm^2). In BALB/c animals, $CD4^+$ and $CD8^+$ T cell depletion experiments were performed using 200 µg anti-CD4 (clone GK1.5) given 1 ×/week (ip) for 6 weeks, or 200 µg anti-CD8 (clone 53–6.7) delivered once (ip) on day 9. In C57BL/6 animals, NK depletion experiments were performed using 200 µg aNK1.1 (PK136, BioXcell)

delivered 1× ip starting the day before therapy. For IFNAR blocking experiments, 200 µg aIFNAR (MAR1-5A3, BioXcell) was delivered on days 9, 13, 17, and 21 (ip) post-tumor implants. For statistical analyses, endpoints were defined as the first time point that tumor area exceeded 250 mm^2 or was non-palpable and did not recur.

Blood, tumor, and lymph node collection and processing

Peripheral blood (PBL) samples were drawn on day 7 post-treatment; 25 µL of fresh heparinized blood was incubated with fluorescence-conjugated antibodies (online supplemental table 2) for 30 min at 4°C in the dark. Tumors were harvested 3 or 7 days post-treatment, cut into small fragments, and digested in 1 mg/mL collagenase and 20 mg/mL DNase (Sigma) in serum-free RPMI-1640 for 30 min at room temperature (RT). TIL were filtered through 70 µm nylon mesh (Cell Treat), washed with 10 mL cRPMI, and collected by centrifugation (1500 rpm, 4 min). Pelleted cells were resuspended for staining and analysis by flow cytometry (see below). Lymph nodes (LNs) were harvested 7 days post-treatment and processed to obtain single-cell suspensions. Red blood cells were lysed with ACK buffer (Lonza) for 2 min at RT. Cells were then rinsed with cRPMI (ThermoFisher) and resuspended for antibody staining.

Flow cytometry

For PBL, TIL, and LN phenotyping, single cell suspensions were stained for 30 min in the dark with combinations of surface markers (online supplemental table 2). Cells were fixed and permeabilized following manufacturer's instructions (FoxP3/Transcription Factor Staining Buffer Set, ThermoFisher, San Diego, CA) and stained with intracellular targets (online supplemental table 2). Flow cytometry data were acquired on an LSR II flow cytometer running FACSDiva software (BD Biosciences), and data were processed and analyzed with FlowJo (BD Biosciences).

Cytokine bead array

PBL was incubated in a 96-well round bottom plate coated with agonistic aCD3/aCD28 (100 µL solution per well of aCD3 (5 µg/mL, 145-2 C11, BD Biosciences) and aCD28 (2 µg/mL, 37.5.1, BD Biosciences)) prior to staining. Plates were incubated for 44 hours in cell culture conditions (37°C, 5% CO_2, 95% humidity) for a cytokine bead array using a ProcartaPlex Mouse Cytokine/Chemokine Panel 1A 36-Plex kit (EPX360-26012-901; Invitrogen). Data were acquired on a Luminex 200 (R&D Systems).

In vitro T cell coculture assays

Cancer cells were plated at a density of 2000 cells/well in a 96-well plate. After 24 hours, adherent cells were rinsed twice with cRPMI supplemented with β-ME. $CD8^+$ T cells were isolated and sorted (BD FACSAria) from CT26 tumors 7 days post-BEMPEG+RT or BEMPEG+NKTR-262 or vehicle control therapy. Isolated $CD8^+$ T cells were added to the cancer cell cultures at a 25:1 effector: target ratio. Cells settled for 15 min at RT prior to hourly tracking of cellular confluence and death (Caspase 3/7 Green Dye, Sartorius) in the Incucyte (Sartorius, Goettingen, Germany), housed at 36.5 C and 5% CO_2 until untreated cells reached confluence. Cancer cell growth and death were analyzed using Zoom software (Incucyte, Sartorius).

Statistical analysis

Data presented in box and whisker plots: the line within the box indicates median, the box spans the IQR, and the whiskers extend to the highest and lowest observations. We used one-way analysis of variance (ANOVA) or repeated measures ANOVA as appropriate along with Šídáks or Dunnett's multiple comparisons tests. Spearman's correlation was used to correlate PBL and TIL populations with tumor size, and Kaplan-Meier plots and log-rank tests were used for tumor survival analysis. All statistical analyses were performed using GraphPad Prism software (GraphPad, San Diego, CA) or R. A $p < 0.05$ was considered significant.

RESULTS

BEMPEG+NKTR-262 improves survival over BEMPEG+RT in a $CD8^+$ T cell-dependent manner

To compare efficacy of BEMPEG +RT against BEMPEG +NKTR-262, we chose two tumor models: CT26 (colon carcinoma) and EMT6 (mammary carcinoma). CT26 allowed us to track tumor-specific (AH1-A5 $tetramer^+$) responses and based on our historical data indicating a 46% survival rate following BEMPEG +RT,[16] there was room to statistically distinguish either an improved or worsened response to BEMPEG +NKTR-262. EMT6 is less responsive to RT and therefore was selected as a secondary tumor model. Tumors were established subcutaneously in the bilateral flanks of BALB/c mice; 10 days later, animals received monotherapies of either 12 Gy RT or 10 µg NKTR-262 in the treated tumor (intratumorally, it) or 0.8 mg/kg BEMPEG (intravenously). For combination therapies, mice received BEMPEG +RT or BEMPEG +NKTR-262. Tumor growth was assessed over time. PBL and, in following experiments, TIL were assessed for phenotype and function 7 days post-treatment (figure 1), which is the peak of the adaptive immune response[4] and before tumor regression impairs our ability to evaluate TIL.

In the treated tumor (right side), we observed a significantly reduced tumor size by day 17 post-treatment following all therapies compared with control (figure 2A–B, $p<0.05$, online supplemental table 1). In the non-treated tumor (left side), we saw a significantly reduced tumor size by day 17 post-treatment only following BEMPEG ($p<0.05$), BEMPEG+RT ($p<0.01$), or BEMPEG+NKTR-262 ($p<0.01$) compared with control (figure 2A–B, online supplemental table 1), demonstrating the systemic influence of BEMPEG on these local therapies. In the non-treated tumor, we observed a significantly larger tumor size after RT, NKTR-262, and BEMPEG in comparison to BEMPEG+NKTR-262

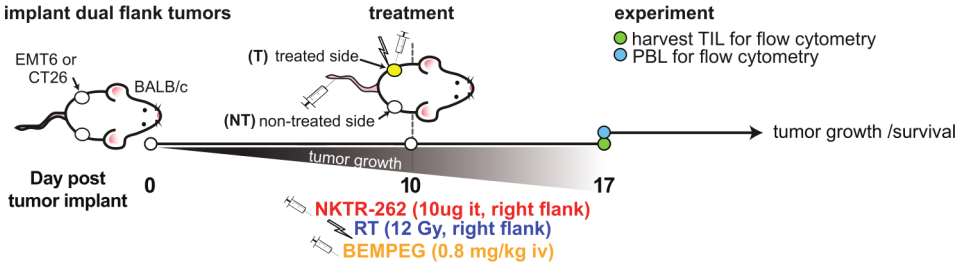

Figure 1 Schematic of treatment and experimental timepoints. For survival experiments, dual flank CT26 or EMT6 tumors were implanted and monitored for growth over time. Monotherapies of right flank RT or NKTR-262 (it) or BEMPEG (iv), or combination therapies of BEMPEG +RT or BEMPEG +NKTR-262 were administered on day 10 post-implant. PBL, LN, or tumors were collected 7 days post-therapy. IT, intratumorally; IV, intravenously; LN, intravenously; PBL, peripheral blood; RT, radiation therapy; TIL, tumor-infiltrating lymphocyte.

(figure 2A–B, p<0.05, online supplemental table 1); the non-treated tumor size was not different comparing the monotherapies to BEMPEG+RT (figure 2A–B, online supplemental table 1). The difference between BEMPEG+NKTR-262 and BEMPEG+RT therapy is seen when comparing the treated and non-treated tumors within each group. There was a significant difference in tumor size between the non-treated and treated tumors after BEMPEG+RT (p<0.05) but not after BEMPEG+NKTR-262, where both non-treated and treated tumors reduced in size at a similar rate (figure 2C). Importantly, most non-treated tumors following BEMPEG+RT grew out (13/15; 86.6%; figure 2A,D), similar to our previous observations.[16] In contrast, many of the non-treated tumors after BEMPEG+NKTR-262 cured. This resulted in significantly increased survival after BEMPEG+NKTR-262 (9/15; 60%) versus BEMPEG+RT (2/15; 13.3%) (figure 2D, p<0.05). We confirmed these results in the EMT6 tumor model (online supplemental figure 1). All surviving mice were tested for tumor-specific memory following rechallenge with CT26 tumors, and all were protected against tumor growth while tumors grew in 100% of control mice (n=0/7 for BEMPEG+NKTR-262; n=0/5 for BEMPEG+RT; n=5/5 untreated control mice).

We previously demonstrated that BEMPEG+RT efficacy depends on $CD8^+$ T cells, with some contribution of NK cells.[16] To address this for BEMPEG+NKTR-262, we performed depletion studies (online supplemental figure 2A) and found that efficacy requires $CD8^+$ T cells (0% survivors) but not $CD4^+$ T cells (37% survivorship vs 36% for BEMPEG+NKTR-262) (figure 2E–F, online supplemental figure 2B). Notably, even without $CD8^+$ or $CD4^+$ T cells, BEMPEG+NKTR-262 therapy induced a significant delay of both treated and non-treated tumor growth in comparison to control (p<0.05 at d14). Because TLR7/8 agonists can activate NK cells directly,[23] we depleted NK cells and determined that NK cells neither influenced overall survival nor eliminated BEMPEG+NKTR-262-delayed tumor growth, as tumor size was still significantly smaller than control by day 13 (p<0.05; online supplemental figure 2C), suggesting BEMPEG+NKTR-262 induced an NK-independent early response (day 1–5) sufficient to delay tumor growth.

BEMPEG+NKTR-262 therapy increases the frequency of activated $CD8^+$ T cells in the PBL in comparison to BEMPEG+RT

Our data suggested that BEMPEG+NKTR-262 induced a more potent systemic $CD8^+$ T cell-dependent antitumor response than BEMPEG+RT; thus, to understand the efficacious systemic response to BEMPEG+NKTR-262, we performed LN (online supplemental figure 3) and PBL (figure 3) immunophenotyping 7 days post-therapy. Focusing on the CT26 model, we examined frequencies of $CD8^+$, NK, $CD4^+FoxP3^+$ T regulatory (Treg), and $CD4^+FoxP3^-$ T effector (Teff) cells, and markers including PD-1, TIM-3, LAG-3, CD62L, ICOS, Ki-67, granzyme A (GzmA), CD25 (IL-2Rα), CD122 (IL-2Rβ), and AH1-A5. In the LN, we found patterns of $CD8^+$ T cell activation, with average frequencies of $CD8^+$ AH1-$A5^+$, $GzmA^+$, IFN-γ^+, and TNF-α^+ all increased 4–5-fold over control after BEMPEG+NKTR-262 but not after BEMPEG+RT (online supplemental figure 3A). Although statistically significant, the overall frequencies of these populations were small. For example, $GzmA^+$ $CD8^+$ T cells ranged from only 1.5%–4.5% after BEMPEG+NKTR-262 (online supplemental figure 3B). Therefore, we focused on PBL for further analysis of peripheral immune responses. For PBL samples, we correlated cell types, phenotypes, and functions with tumor size across treatment groups (figure 3A). We found no significant correlations between PBL phenotypes and treated tumor size; however, we found many significant negative correlations (p<0.05) between $CD8^+$ T cell markers and non-treated tumor size, including $ICOS^+$, AH1-$A5^+$, PD-1^+, Ki-67^+, and $GzmA^+$ (figure 3A), which highlights the value of the peripheral response in monitoring the non-treated tumor response. Comparing $CD8^+$ T cell phenotypes between treatment groups revealed that BEMPEG+NKTR-262 significantly expanded $CD8^+$ T cells over BEMPEG+RT (figure 3B,D; p<0.0001). The $CD8^+$ T cell phenotypes that significantly distinguished BEMPEG+NKTR-262 from BEMPEG+RT were PD-1, CD122, GzmA, ICOS, and Ki-67 (for all: p<0.0001), indicating that BEMPEG+NKTR-262 is superior to BEMPEG+RT at expanding active functional $CD8^+$ T cells (figure 3B–D).

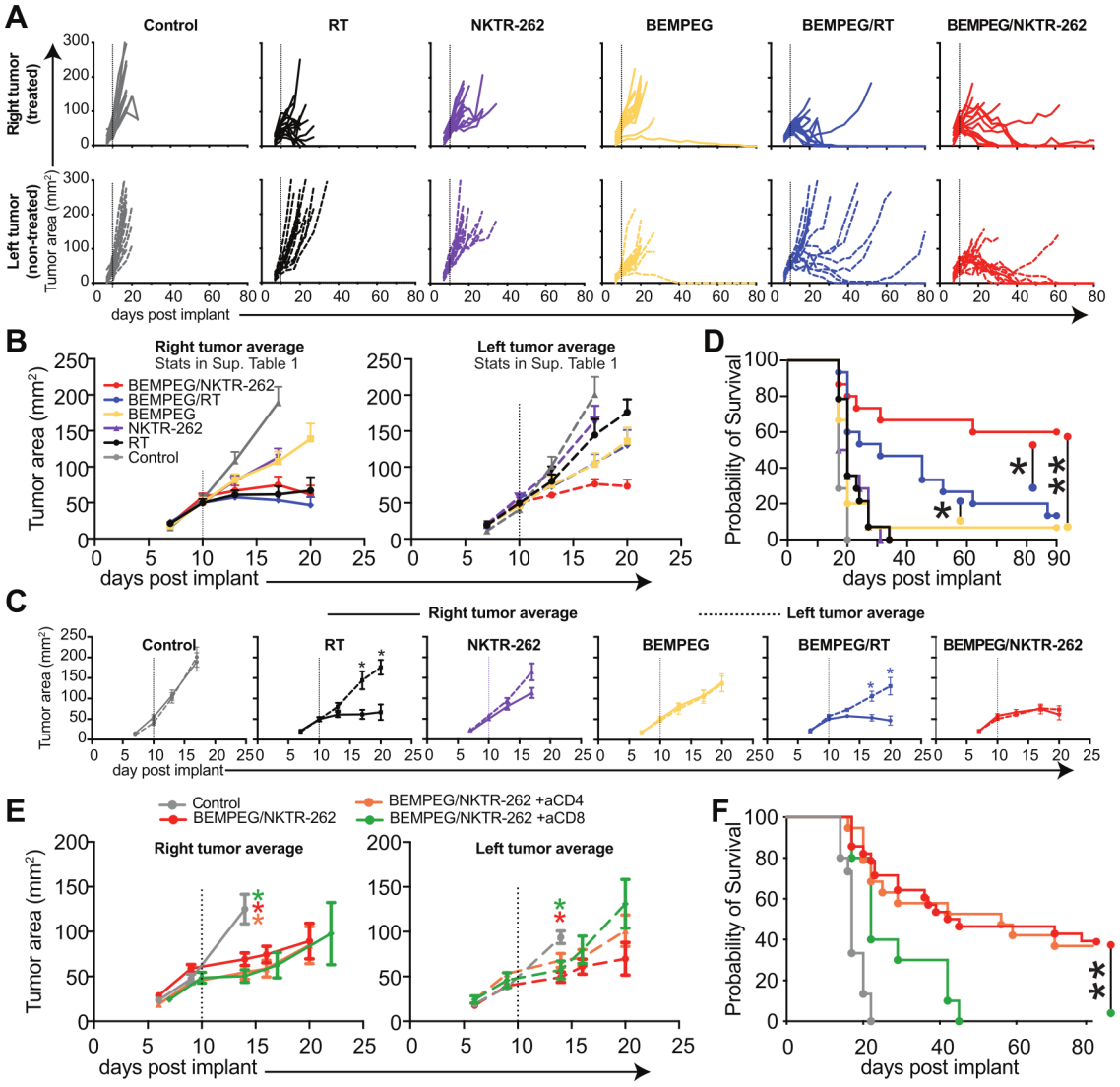

Figure 2 BEMPEG +NKTR-262 combination therapy significantly reduces tumor growth. (A) CT26 tumor growth depicted for individual animals on the right side (treated) tumor (top row, solid lines), the left side (non-treated) tumor (middle row, dashed lines). (B) Averages for the right and left side tumor growth for each treatment group (; average growth curve lines end after first mouse in the group reached tumor growth cut-off). Dotted line indicates treatment day. Repeated measures ANOVA statistics are presented in online supplemental table 1. (C) Average tumor growth from right (solid line) and left (dotted line) tumors for each group. Statistics indicate comparisons between the right and left tumors within each group. Repeated measures ANOVA. (D) Probability of survival for BEMPEG +NKTR-262 (red), BEMPEG +RT (blue), BEMPEG (yellow), NKTR-262 (purple triangle), RT (black circle), and control (gray). Log-rank test. For A–D, N=14 or 15 from two independent experiments. *P<0.05, **p<0.01. (E) Average CT26 tumor growth after BEMPEG +NKTR-262 therapy in the absence of $CD8^+$ T cells (green) or $CD4^+$ T cells (orange). Repeated measures ANOVA, colored asterisks indicate group that is different from control. (F) Probability of survival for control (gray), BEMPEG +NKTR-262 (red), BEMPEG +NKTR-262+aCD8 (green), and BEMPEG +NKTR-262+aCD4 (orange). **P<0.01, log-rank test. For (E, F), N=10–20 from two independent experiments. ANOVA, analysis of variance; RT, radiation therapy.

Teff and Treg populations did not have many differences between combination treatment groups because many phenotypes were driven by BEMPEG and not altered by additional therapy (online supplemental figure 4A). However, $CD25^+$ and $ICOS^+$ frequencies were significantly increased in Teff and Treg after both BEMPEG monotherapy and BEMPEG+NKTR-262 combination therapy in comparison to BEMPEG+RT, suggesting a negative effect of RT on these phenotypes (online supplemental figure 4A).

To determine whether these therapies altered Th1/Th2 polarization, we analyzed serum cytokine levels via multiplex ELISA. We found an increase in IFN-g (Th1) and a decrease in IL-4 (Th2) and IL-3 (immune regulating cytokine), suggesting a more inflammatory helper T cell response in the periphery after BEMPEG+NKTR-262 in comparison to BEMPEG+RT (online supplemental figure 4B). Other proinflammatory cytokines induced by BEMPEG and significantly elevated after BEMPEG+NKTR-262 compared with BEMPEG+RT included IL-1β,

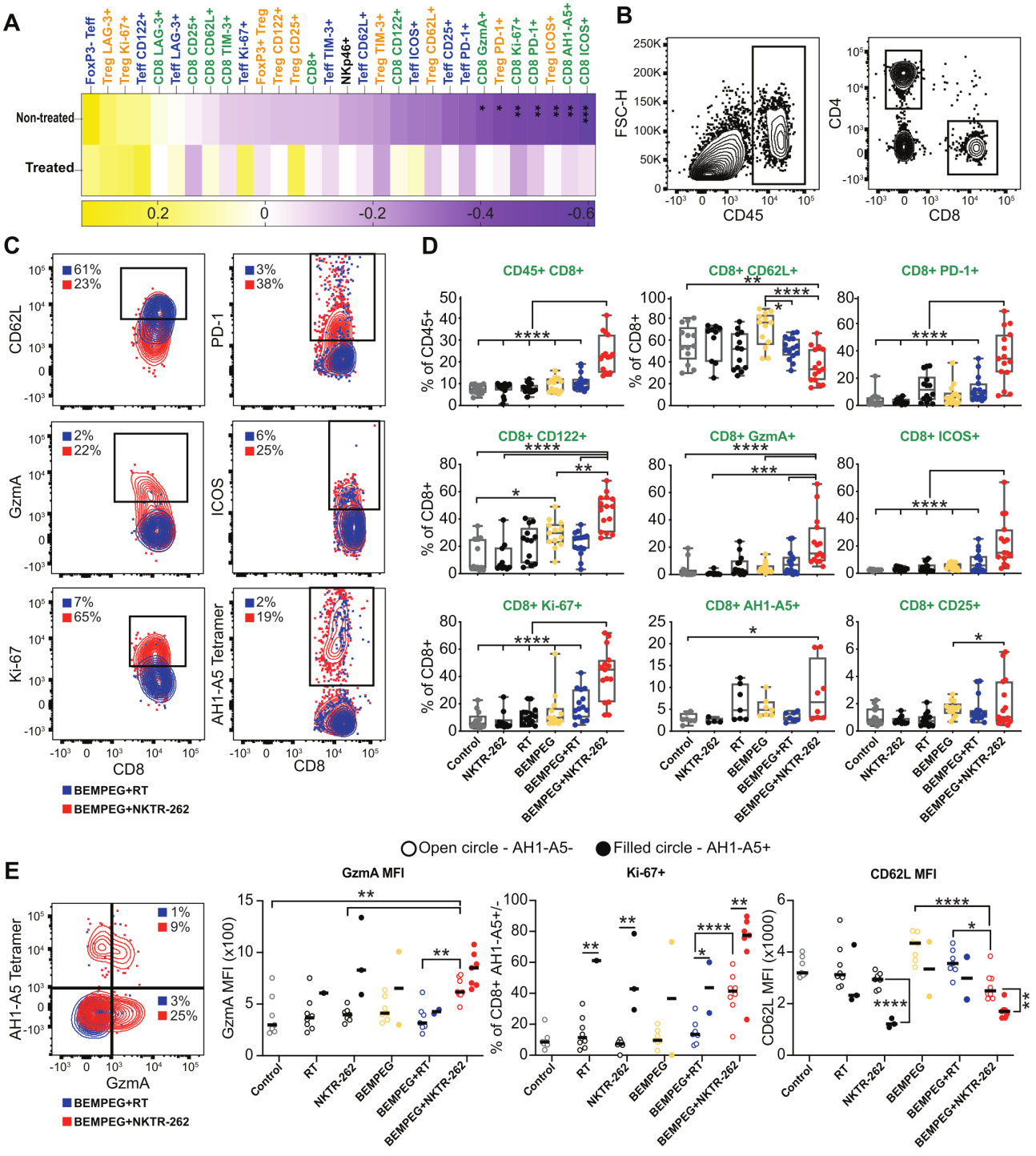

Figure 3 BEMPEG+NKTR-262 induces a greater expansion of active CD8$^+$ T cells than BEMPEG+RT. (A) We determined immune phenotypes from PBL 7 days post-therapy. These data are presented as Spearman correlations of PBL phenotypes with tumor size, across individuals and treatment groups. Significant correlations after FDR correction are indicated. (B) Representative flow cytometry plots of CD45$^+$, CD4$^+$, and CD8$^+$ gates. (C) Representative flow cytometry plots demonstrating CD8$^+$ cell expression of CD62L, PD-1, GzmA, ICOS, Ki-67, and AH1-A5 after BEMPEG+RT (blue) or BEMPEG+NKTR-262 (red). (D) PBL immune phenotypes determined by flow cytometry. Box and whisker plots represent the min and max (whiskers), the quartiles (box) and median (line). Each point represents an individual mouse. N=10–20, from two independent experiments, except AH1-A5, which is one of two representative experiments N=4–8 per experiment. One-way ANOVA with Šídáks multiple comparisons test. (E) (Left) Representative flow cytometry plot showing AH1-A5$^+$ and GzmA$^+$ CD8$^+$ T cells. (right) Granzyme A (GzmA), proliferation (Ki-67), and CD62L expression on tumor specific (AH1-A5$^+$, filled circle) or not (AH1-A5$^-$, open circle). Only mice that had more than 70 AH1-A5$^+$ cells were analyzed for AH1-A5$^+$ phenotypes. Data from one of two representative experiments. For comparisons between AH1-A5$^{+/-}$ within one treatment group, Student's t-test. For comparisons among treatment groups, one-way ANOVA with Šídáks multiple comparisons test. *P<0.05, **p<0.01, ***p<0.001, ****p<0.0001. ANOVA, analysis of variance; FDR, false discovery rate; PBL, peripheral blood; RT, radiation therapy.

IL-1α, GM-CSF, and RANTES (CCL5) (online supplemental figure 4B), which are associated with the inflammatory process and leukocyte recruitment, further supporting that BEMPEG+NKTR-262 induces an immune response that supports antitumor immunity.

AH1-A5$^+$ CD8$^+$ T cells were expanded over control in 50% of the mice that received BEMPEG+NKTR-262 therapy, but not expanded over control in any mice after BEMPEG+RT; however, statistically there was no difference between combination therapies (figure 3D). Due to the lack of difference in AH1-A5$^+$ CD8$^+$ T cell frequency between the two combination therapies, we thought there may have been a broadening of the tumor-specific TCR repertoire after BEMPEG+NKTR-262 therapy due to NKTR-262-induced antigen presenting cell (APC) differentiation. Therefore, we examined AH1-A5$^+$ and AH1-A5$^-$ CD8$^+$ T cells in depth, hypothesizing that tumor-specific AH1-A5$^-$ cells would express similar levels of activation markers as AH1-A5$^+$. Indeed, we found similar frequencies of proliferating (Ki-67$^+$) AH1-A5$^-$ cells after BEMPEG+NKTR-262 as of AH1-A5$^+$ after BEMPEG+RT and significantly more proliferating AH1-A5$^-$ CD8$^+$ T cells after BEMPEG+NKTR-262 than BEMPEG+RT ($p<0.0001$; figure 3E). Furthermore, GzmA MFI was statistically indistinguishable comparing AH1-A5$^+$ to AH1-A5$^-$ CD8$^+$ T cells from BEMPEG+NKTR-262-treated tumors, and GzmA MFI from AH1-A5$^-$ CD8$^+$ T cells after BEMPEG+NKTR-262 was significantly increased in comparison to AH1-A5$^+$ CD8$^+$ T cells after BEMPEG+RT ($p<0.01$) (figure 3E). Similarly, CD62L MFI (figure 3E), was significantly reduced in AH1-A5$^-$ CD8$^+$ T cells after BEMPEG+NKTR-262 compared with BEMPEG+RT ($p<0.05$). This data could suggest that the BEMPEG+NKTR-262 induced AH1-A5$^-$ CD8$^+$ T cells were activated 'bystander' CD8$^+$ T cells[24] driven by proinflammatory cytokines such as type I interferons (IFN) induced by TLR agonists, or that they were activated tumor-specific CD8$^+$ T cells that targeted a different tumor antigen, perhaps an indication of increased priming after BEMPEG+NKTR-262 therapy.

IFN-α/β signaling contributes to BEMPEG+NKTR-262 efficacy

Type I IFN signaling supports bystander CD8$^+$ T cell activation and drives increased cross-priming capacity of dendritic cells (DCs) after RT,[25] therefore, we blocked the IFN alpha/beta receptor (IFNAR-1) to ask what role IFN signaling plays in the context of BEMPEG+NKTR-262 therapy. IFNAR signaling contributed to BEMPEG+NKTR-262 efficacy, as IFNAR blockade reduced survival from 80% to 50% (figure 4) primarily due to increased growth of non-treated tumors (online supplemental figure 5). Examination of PBL immune phenotypes 7 days post-treatment revealed that IFNAR signaling contributed to CD8$^+$ T cell expansion ($p<0.0001$) and effector function (GzmA$^+$, ICOS$^+$, PD-1$^+$, CD62L^{lo}) (figure 4B). In all cases the influence of type I IFN signaling was significant for BEMPEG+NKTR-262 and not for BEMPEG+RT (figure 4).

We observed reduced AH1-A5$^+$ CD8$^+$ T cell frequency after BEMPEG+RT plus IFNAR blockade that did not reach statistical significance (figure 4B). However, AH1-A5$^+$ CD8$^+$ T cell frequency was significantly reduced after BEMPEG+NKTR-262 plus IFNAR blockade (figure 4B, $p<0.01$), which may reflect the contribution of IFN-α/β signaling to cross-presentation of tumor antigens. Interestingly, BEMPEG+NKTR-262 induced significantly more AH1-A5$^+$ cells than BEMPEG+RT in the absence of type I IFN signaling ($p<0.01$), yet AH1-A5$^+$ CD8$^+$ T cells had similar frequencies of CD62L^{lo}, GzmA$^+$, and Ki-67$^+$ in the presence or absence of IFNAR signaling across combination therapies (figure 4C), suggesting type I IFNs do not influence AH1-A5$^+$ CD8$^+$ T cell function. However, for AH1-A5$^-$ CD8$^+$ T cells, frequencies of GzmA$^+$, Ki-67$^+$, and PD-1$^+$ CD8$^+$ T cells were significantly decreased after BEMPEG+NKTR-262 plus IFNAR blockade (figure 4D), indicating type I IFNs influenced the function of AH1-A5$^-$ CD8$^+$ T cells after BEMPEG+NKTR-262. This pattern did not occur after BEMPEG+RT. Collectively, these data suggest two results: first, unlike BEMPEG+RT, BEMPEG+NKTR-262-induced type I IFN signaling likely leads to increased priming/cross-priming; and second, BEMPEG+NKTR-262-induced type I IFN signaling supports a highly functional AH1-A5$^-$ CD8$^+$ T cell population that may be comprised of activated bystander cells or non-AH1-specific tumor-reactive cells.

Both TLR signaling and type I IFNs can induce DC maturation and regulate priming.[26] Because BEMPEG +NKTR-262 efficacy relies, in part, on type I IFNs to induce tumor-specific CD8$^+$ T cells (figure 4B), we asked whether we could detect differences in the DC compartment comparing BEMPEG +NKTR-262 and BEMPEG +RT. We harvested CT26 tumors 3 days post-treatment and analyzed DC (CD11c$^+$MHCII$^+$CD24$^+$F4/80$^-$) phenotypes (CD103, PD-L1, Arg1, iNOS) by flow cytometry. The UMAP distribution of DCs (online supplemental figure 6A) and an unbiased clustering algorithm (FlowSOM) (online supplemental figure 6B) revealed that BEMPEG drove a significantly different distribution of DCs, with a majority of DCs in cluster 0 for the three treatment groups that received BEMPEG (online supplemental figure 6B). Within cluster 0, BEMPEG +NKTR-262 treatment induced higher MHCII and CD103 expression than BEMPEG +RT (online supplemental figure 6C), both markers of conventional type 1 DC maturation (cDC1).[26 27] CD103$^+$ DC frequency was driven by both BEMPEG and NKTR-262 on the treated side, but not by RT (online supplemental figure 6D). Thus, BEMPEG +NKTR-262 resulted in a synergistic increase in CD103$^+$ DC frequency over BEMPEG +RT

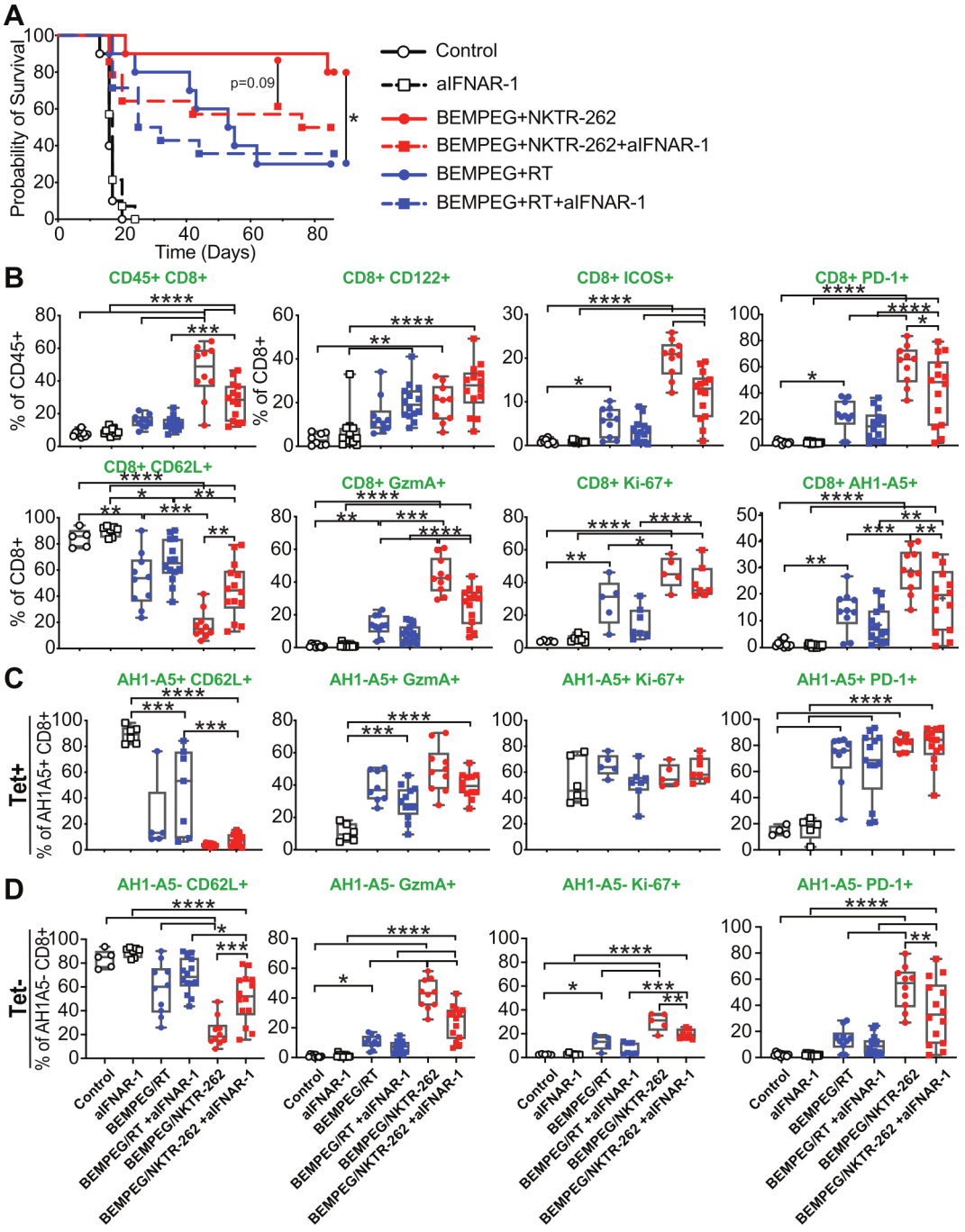

Figure 4 IFNα/β signaling contributes to efficacy of BEMPEG+NKTR-262 therapy. (A) Probability of survival with CT26 tumors in WT mice (open circle), WT mice with aIFNAR-1 antibody (open square), BEMPEG+NKTR-262 (red circle), BEMPEG+NKTR-262 with aIFNAR-1 antibody (red square), BEMPEG+RT (blue circle), or BEMPEG+RT with aIFNAR-1 antibody (blue square). *P<0.05, log-rank test. (B) PBL immune phenotyping 7 days post-therapy. One-way ANOVA with Šídáks multiple comparisons test. (C) CD62L, GzmA, and Ki-67 expression on tumor specific, AH1-A5^{+} cells. (D) CD62L, GzmA, and Ki-67 expression on AH1-A5^{-} cells. ANOVA with Šídáks multiple comparisons test. For A–D, N=10–14 from two independent experiments, for some markers, one representative of the two experiments is shown. ANOVA, analysis of variance; PBL, peripheral blood.

(online supplemental figure 6D). These data suggest BEMPEG +NKTR-262 induces a greater cDC1 frequency than BEMPEG +RT, which may support increased T cell priming.

On further assessment of NKTR-262's impact on innate immune responses in the tumor microenvironment (TME), we found a pattern of changes driven by NKTR-262 on day 1 post-treatment that were maintained by BEMPEG on day 3. These changes included an increased ratio of M1-like (iNOS^{+}) to M2-like (Arginase^{+}) macrophages and an increased frequency of PD-L1 +macrophages (online supplemental figure 7A). Other NKTR-262-driven changes to the TME included a reduced frequency of monocytic MDSCs

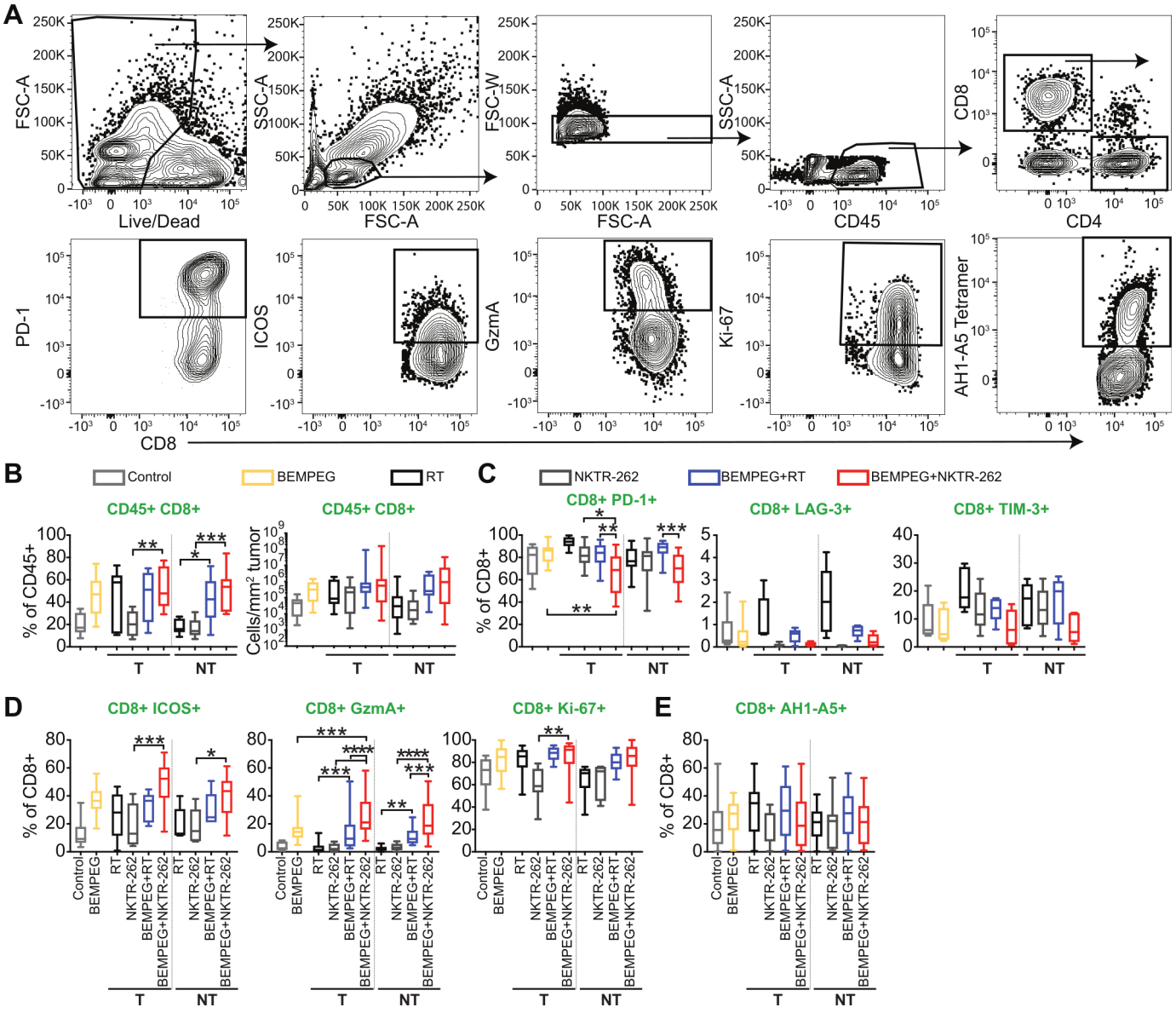

Figure 5 BEMPEG+NKTR-262 treatment induces CD8⁺ T cells in the tumor with reduced checkpoint receptor expression and increased functional marker expression than BEMPEG+RT. (A) Representative flow cytometry gating strategy for CT26 tumors harvested 7 days post-therapy. (B) Percent (left) and density (right) of CD8⁺ T cells in the tumor. N=8–18, from three or four independent experiments. (C) Checkpoint receptors expressed on CD8⁺ T cells in the tumor. N=15 for PD-1 (from three experiments), 5 for Tim-3 and LAG-3 (from one experiment). (D) Activation markers expressed on CD8⁺ T cells in the tumor. For ICOS, N=5–9 from two experiments; for GzmA, N=13–23 from four experiments; for Ki-67, N=9–13 from three experiments. (E) Frequency of AH1-A5⁺ CD8⁺ T cells. N=15–20 from four experiments. For comparisons among treatment groups, one-way ANOVA with Šídáks multiple comparisons test. *P<0.05, **p<0.01, ***p<0.001, ****p<0.0001. NT, non-treated tumor; RT, radiation therapy; T, treated tumor.

and increased frequency of polymorphonuclear MDSCs (online supplemental figure 7B). Taken with the observed increase in cDC1s, these results suggest an 'antitumor' TME that may better support an active adaptive immune response.

BEMPEG+NKTR-262 induces CD8⁺ T cells with reduced checkpoint receptor expression and increased functional marker expression as compared with BEMPEG+RT

We next looked at TIL phenotypes and functions from the treated and non-treated tumors 7 days post-therapy by flow cytometry (figure 5A). There was no significant difference in CD8⁺ T cell frequency or density (cells/mm²) in the treated or non-treated tumors at this timepoint after BEMPEG+NKTR-262 compared with BEMPEG+RT (figure 5B), though there was a significant increase in Teff and concomitant decrease in Treg frequency in the treated tumor after BEMPEG+NKTR-262 compared with BEMPEG+RT (p<0.05, online supplemental figure 8A,B). Those changes in frequency were not reflected

in Teff and Treg density (online supplemental figure 8A,B).

CD8$^+$ TIL had reduced checkpoint receptor expression and increased functional marker expression after BEMPEG+NKTR-262 compared with BEMPEG+RT (figure 5C). For example, PD-1$^+$ CD8$^+$ T cell frequency was significantly decreased after BEMPEG+NKTR-262 compared with BEMPEG+RT in the treated and non-treated tumors (p<0.01), and exhaustion markers LAG-3$^+$ and TIM-3$^+$ were slightly decreased (figure 5C). GzmA$^+$ CD8$^+$ T cells were significantly increased after BEMPEG+NKTR-262 compared with BEMPEG+RT in the treated and non-treated tumors (p<0.001, figure 5D), while the activation/proliferation markers ICOS$^+$ and Ki-67$^+$ trended higher in CD8$^+$ T cells after BEMPEG+NKTR-262 compared with BEMPEG+RT. These changes were specific to CD8$^+$ T cells and not observed in Teff or Treg cells (online supplemental figure 8C,D). Consistent with the minimal difference observed between the combination therapies in peripheral AH1-A5$^+$ CD8$^+$ T cells, we found no difference in AH1-A5$^+$ CD8$^+$ T cell frequency in the tumor (figure 5E). The increase in GzmA$^+$ CD8$^+$ T cells coupled with the decrease in PD-1$^+$ CD8$^+$ T cells in the TME suggests that BEMPEG+NKTR-262 supports increased cell activation and function as compared with BEMPEG+RT.

BEMPEG+NKTR-262 induces CD8$^+$ T cells with greater cytotoxic capacity than BEMPEG+RT

Because BEMPEG+NKTR-262 induced more GzmA$^+$ CD8$^+$ T cells than BEMPEG+RT, regardless of AH1-A5 status, we hypothesized that increased priming after BEMPEG+NKTR-262 led to an increased proportion of tumor-specific CD8$^+$ T cells. To test this hypothesis, we used transgenic Nur77 reporter mice in which the strength of TCR stimulation correlates with GFP expression.[22] Surprisingly, Nur77$^+$ CD8$^+$ T cell frequency after BEMPEG+NKTR-262 was similar to BEMPEG+RT (figure 6A, left), which suggests that there was not an increased proportion of TCR-stimulated CD8$^+$ T cells at this timepoint. However, after BEMPEG+NKTR-262, a significantly greater proportion of Nur77$^+$ cells expressed GzmA in the treated tumor than their BEMPEG+RT-treated counterparts (figure 6A, right). Therefore, we

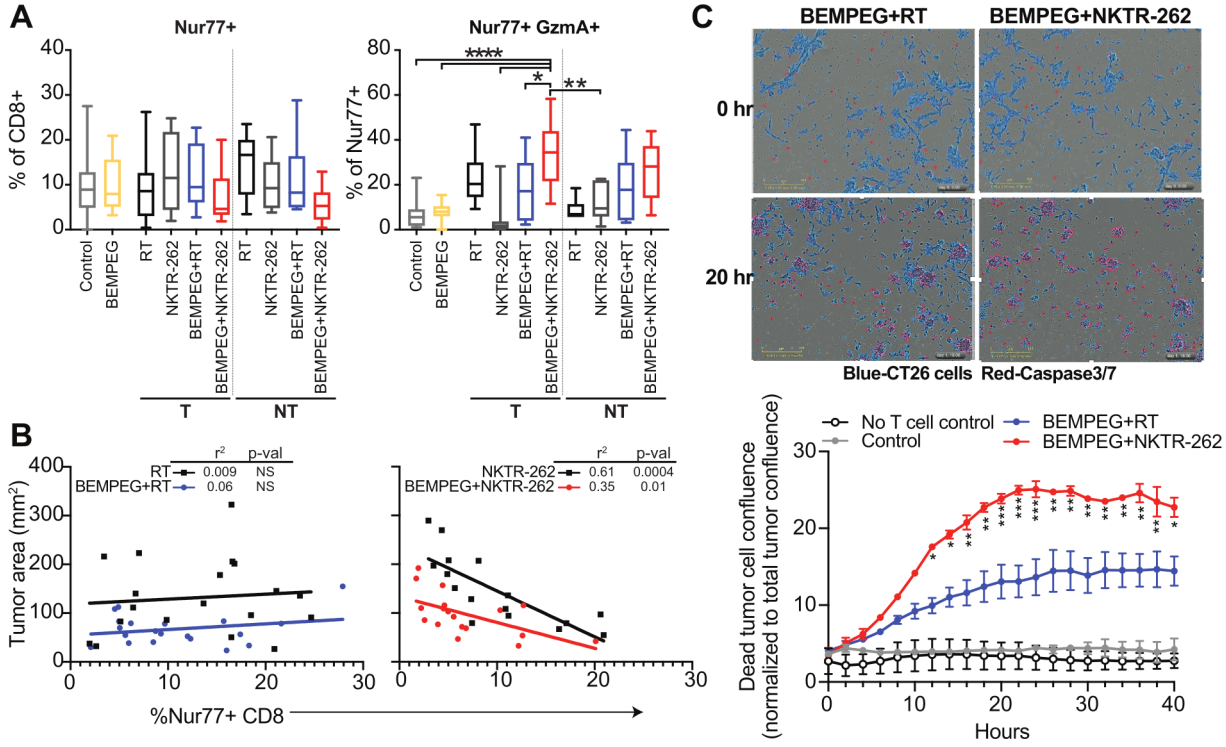

Figure 6 BEMPEG+NKTR-262 induces CD8$^+$ T cells with greater cytotoxic capacity than BEMPEG+RT. (A) Percent of Nur77$^+$CD8$^+$ T cells in the tumor 7 days post-treatment (left). Percent of GzmA$^+$ Nur77$^+$CD8 T cells in the tumor 7 days post-treatment (right). N=8–14 from two independent experiments. One-way ANOVA with Šídáks multiple comparisons test. *p<0.05, **p<0.01, ****p<0.0001. (B) Correlation between percent of Nur77$^+$ CD8$^+$ T cells and tumor area for either RT monotherapy (black square, left), BEMPEG+RT (blue circle, left), NKTR-262 monotherapy (Black square, right), or BEMPEG+NKTR-262 (red circle, right). Each point represents either a treated or non-treated tumor from a mouse that received the indicated therapy. N=16–19, tumors from two independent experiments. Simple linear regression. (C) Incucyte assay of CD8$^+$ T cells isolated from CT26 tumors 7 days post-treatment incubated with CT26 cells in vitro for 40 hours. Tumor cell apoptosis was tracked by size and Caspase 3/7 staining; representative images of each condition are shown (top). Quantification of the dead (caspase3/7$^+$) CT26 cells per total cell confluence over time. Data from one of three independent experiments shown (Bottom). *P<0.05, repeated measures ANOVA with Dunnett's multiple comparison test. ANOVA, analysis of variance; NT, non-treated tumor; RT, radiation therapy; T, treated tumor.

hypothesized that BEMPEG+NKTR-262 induced more potent cytotoxic function on a per cell basis as compared with BEMPEG+RT.

To test this, we asked whether Nur77$^+$ CD8$^+$ T cells correlated with tumor area (figure 6B). On examining treated and non-treated tumors from RT or NKTR-262-treated mice separately, we observed that Nur77$^+$ T cell frequency did not correlate with tumor size after RT. In contrast, increased Nur77$^+$ T cell frequency correlated with reduced tumor size in both treated and non-treated tumors after NKTR-262 (online supplemental figure 9). Therefore, we combined the treated and non-treated tumors for further analysis. We saw no correlation between Nur77$^+$ CD8$^+$ T cell frequency and tumor size after BEMPEG+RT (figure 6B, left); however, Nur77$^+$ CD8$^+$ T cell frequency significantly correlated with tumor size after BEMPEG+NKTR-262 (figure 6B, right). Because higher Nur77$^+$ frequency correlated with smaller tumor size, we hypothesized that BEMPEG+NKTR-262 induced more potent CD8$^+$ T cell cytotoxic function. To test this hypothesis, we sorted CD8$^+$ T cells from treated and non-treated tumors and measured their cytolytic activity against autologous CT26 cells in vitro. BEMPEG+NKTR-262 elicited significantly increased CD8$^+$ T cell cytolytic capacity compared with BEMPEG+RT (figure 6C). Taken together, these data demonstrate that BEMPEG+NKTR-262 induced and recruited to the tumor activated CD8$^+$ T cells that were characterized by increased GzmA and greater cytolytic capacity than those generated by BEMPEG+RT.

DISCUSSION

Combining drugs with complementary mechanisms of action, such as chemotherapy regimens in hematological malignancies and breast cancer,[28] can improve therapeutic outcomes. However, determining the combinations that will achieve optimal clinical responses is an ongoing and unresolved question. Herein, we compared the IL-2 agonist prodrug BEMPEG[3 4] in combination with either RT or the TLR agonist NKTR-262 and found that in multiple mouse models of multifocal disease, BEMPEG+NKTR-262 resulted in significantly slower tumor growth, specifically in non-treated tumors, and increased survival in comparison to BEMPEG+RT. Both combinations rely on CD8$^+$ T cells for efficacy; however, BEMPEG+NKTR-262 induces more potent tumor-specific cytotoxic CD8$^+$ T cells than BEMPEG+RT.

One feature that defines the immune response to BEMPEG is the preferential expansion of CD8$^+$ and CD4$^+$ Teff cells over Tregs in tumor tissue.[3 4] This attribute of BEMPEG has the potential to mechanistically synergize with other therapies capable of alleviating T cell exhaustion, like immune checkpoint blockade (ICB), and/or with therapies that evoke new antitumor responses, like RT or TLR agonists. Indeed, BEMPEG has shown synergy in combination with ICB preclinically[3 4] and clinically[29 30] (NCT02983045, NCT03138889, NCT03635983). BEMPEG/ICB-mediated synergy occurs through BEMPEG-driven Treg reduction and tumor-specific T cell expansion in the tumor,[3 4] which are prevented from reaching exhaustion by ICB. By comparison, RT increases TIL Treg frequency,[20] and as a result, BEMPEG+RT reduces the favorable Teff:Treg ratio driven by BEMPEG in comparison to BEMPEG monotherapy.[16 20] Interestingly, we found BEMPEG+NKTR-262 significantly increased TIL CD4$^+$ Teff frequency as compared with BEMPEG+RT. While CD4$^+$ T cell depletion did not influence BEMPEG+RT[16] or BEMPEG+NKTR-262 efficacy, given the favorable Teff:Treg ratio and shift towards Th1 polarization after BEMPEG+NKTR-262, it is likely that these CD4$^+$ T cell phenotypes contribute to a TME that supports CD8$^+$ T cell differentiation and function. Further, maintenance of the BEMPEG-induced Teff:Treg ratio following the inclusion of NKTR-262 suggests compatible mechanistic synergy between these two modalities.

One challenge for improving immunotherapy efficacy is inducing new antitumor immune responses. A key step in the initiation of new antitumor immunity is cross-presentation of tumor antigens by DCs and other professional APCs. Both RT and TLR ligands can induce DC maturation through pro-inflammatory signals. RT primarily provokes local proinflammatory signals through tumor cell death, which can be immunogenic or tolerogenic depending on a myriad of factors including cell cycle phase, cell type, and microenvironmental factors like hypoxia.[31] Further, RT-induced DC maturation depends on the TME: radioimmunogenic tumors support cDC1 activation, while non-radioimmunogenic tumors do not.[27] Additionally, preexisting immunity is required for RT-induced immune responses.[12] Thus, BEMPEG+RT therapy likely expands and activates an existing population of tumor-reactive T cells and, at least in preclinical models, does not induce new antitumor responses.

In contrast to RT, intratumoral delivery of TLR agonists may generate new antitumor responses through APC activation. TLR7/8 agonists are particularly interesting as plasmacytoid DCs, B cells, monocytes, and myeloid DCs all express TLR7/8, allowing agonists to activate a wide-ranging group of APCs.[32] Further, TLR7/8 agonists can induce tumor cell death through activated tumoricidal DCs.[33] Thus, we hypothesized that NKTR-262 provides more potent immunogenic proinflammatory signals required for DC activation than RT. Indeed, 3 days post-treatment, BEMPEG changed the dominant DC phenotype, likely to a more mature phenotype, as IL-2 signaling indirectly drives DC expansion.[34] Combination with NKTR-262 further boosted this DC population, as after BEMPEG+NKTR-262 therapy DCs exhibited an expanded CD103$^+$ population in comparison to BEMPEG+RT. We also detected increased CCL5 (RANTES) and GM-CSF in the serum after BEMPEG+NKTR-262, both cytokines that promote leukocyte migration; given that migration follows a gradient, we speculate increased levels of these cytokines in the tumor. Further, our data suggest

BEMPEG+NKTR-262 preferentially expands and/or increases cDC1 recruitment and influences macrophage polarization. While we focused on comparing different innate immune stimulators paired with BEMPEG, combining RT with a TLR7/8 agonist has shown DC-based synergistic effects in mouse models.[35] Thus, the triple combination of RT, NKTR-262, and BEMPEG would be interesting to pursue in the future.

Type I IFNs can stimulate immune responses by activating DCs through promoting cross-presentation and by activating $CD8^+$ T cell effector function.[36] In addition to BEMPEG+NKTR-262 more effectively inducing cDC1 maturation in the CT26 model than BEMPEG+RT, we found an increased dependence on IFNα/β signaling for BEMPEG+NKTR-262 over BEMPEG+RT. We note that RT dependence on IFNα/β signaling depend on the tumor model and RT dose applied,[37] with fractionated doses inducing a greater abscopal effect.[38] BEMPEG+NKTR-262 induced IFNα/β-signaling contributed to priming, as the proportion of AH1-$A5^+$ cells was reduced in its absence. We also observed a significant reduction in $GzmA^+$ and Ki-67^+ AH1-$A5^-$ $CD8^+$ T cell frequency in the absence of IFNα/β signaling, which may be bystander $CD8^+$ T cells. Highly cytolytic activated bystander $CD8^+$ T cells induced by anti-CD40 and IL-2 can drive antitumor effects[39] and, in viral infections, the bystander response is rapidly induced by type I IFNs and TLR agonists to control infection before the antigen-specific T cell response.[24 40] We observed early control of tumor growth after BEMPEG+NKTR-262, which could reflect rapidly activated bystander $CD8^+$ T cells. While intratumoral bystander $CD8^+$ T cells are found in human cancers,[41] their role is not yet understood. Our findings suggest that bystander $CD8^+$ T cells may contribute to highly efficacious antitumor immune responses induced by BEMPEG+NKTR-262.

Our data demonstrate that BEMPEG +NKTR-262 and BEMPEG +RT treatments lead to similar patterns of T cell trafficking to the tumor and frequencies of AH1-$A5^+$ $CD8^+$ T cells. However, BEMPEG +NKTR-262 increased $CD8^+$ T cell cytotoxic capacity and induced significantly more activated ($GzmA^+$) $Nur77^+$ $CD8^+$ T cells over BEMPEG +RT, which may explain the greater antitumor effects of BEMPEG +NKTR-262 even in the absence of an increase in total AH1-$A5^+$ $CD8^+$ T cells. Whether the highly cytotoxic antitumor immune response generated by BEMPEG +NKTR-262 requires pre-existing immunity or if it is induced de novo following BEMPEG +NKTR-262-induced DC maturation will be an important question to address in future work. These data provide an insight into the mechanisms by which BEMPEG +NKTR-262 augments antitumor immunity and a establish a framework to explore whether similar mechanisms regulate tumor-specific responses in patients with locally advanced or metastatic solid tumors currently being treated with NKTR-262 in combination with BEMPEG and anti-PD-1 (nivolumab) (NCT03435640).

Twitter Annah S Rolig @annahrolig and William L Redmond @WWredmond4

Acknowledgements The authors would like to acknowledge the EACRI Flow Cytometry Core Facility, EACRI Cancer Research Animal Division (CRAD), and the NIH Tetramer Core Facility for providing AH1-A5 tetramers.

Contributors ASR made substantial contributions to the conception, design, data analysis and interpretation, and drafted the manuscript. DCR and GHM made substantial contributions to data acquisition and analysis. SK and WR provided key reagents and contributed to the conception and design of the experiments. WLR made substantial contributions to the conception, design, data analysis and interpretation, drafted the manuscript, and is responsible for the overall content as guarantor. All authors have reviewed and approved the submitted manuscript.

Funding Funding was provided by Nektar Therapeutics and Providence Portland Medical Foundation.

Competing interests Redmond: Research support from Galectin Therapeutics, Bristol Myers Squibb, GlaxoSmithKline, MiNA Therapeutics, Inhibrx, Veana Therapeutics, Aeglea Biotherapeutics, Shimadzu, OncoSec, and Calibr. Patents/Licensing Fees: Galectin Therapeutics. Advisory Boards: Nektar Therapeutics, Vesselon. Rubas: Former employee of Nektar Therapeutics; current employee of Sutra Biopharma. Kivimäe: Current employee of Nektar Therapeutics. All other authors had no relevant disclosures.

Patient consent for publication Not applicable.

Ethics approval Experimental procedures were performed according to the National Institutes of Health Guide for the Care and Use of Laboratory Animals and in accordance with the EACRI Institutional Animal Care and Use Committee (Animal Welfare Assurance No. A3913-01).

Provenance and peer review Not commissioned; externally peer reviewed.

Data availability statement All data relevant to the study are included in the article or uploaded as online supplemental information.

ORCID iDs
Annah S Rolig http://orcid.org/0000-0001-7080-4352
William L Redmond http://orcid.org/0000-0002-2572-1731

REFERENCES

1 Mellman I, Coukos G, Dranoff G. Cancer immunotherapy comes of age. *Nature* 2011;480:480–9.
2 Waldman AD, Fritz JM, Lenardo MJ. A guide to cancer immunotherapy: from T cell basic science to clinical practice. *Nat Rev Immunol* 2020;20:651–68.
3 Sharma M, Khong H, Fa'ak F, *et al*. Bempegaldesleukin selectively depletes intratumoral Tregs and potentiates T cell-mediated cancer therapy. *Nat Commun* 2020;11.
4 Charych DH, Hoch U, Langowski JL, *et al*. NKTR-214, an engineered cytokine with biased IL2 receptor binding, increased tumor exposure, and marked efficacy in mouse tumor models. *Clin Cancer Res* 2016;22:680–90.
5 Charych D, Khalili S, Dixit V, *et al*. Modeling the receptor pharmacology, pharmacokinetics, and pharmacodynamics of NKTR-214, a kinetically-controlled interleukin-2 (IL2) receptor agonist for cancer immunotherapy. *PLoS One* 2017;12:e0179431.
6 Atkins MB, Lotze MT, Dutcher JP, *et al*. High-Dose recombinant interleukin 2 therapy for patients with metastatic melanoma: analysis of 270 patients treated between 1985 and 1993. *J Clin Oncol* 1999;17:2105.

7 Rosenberg SA, Yang JC, Topalian SL, *et al*. Treatment of 283 consecutive patients with metastatic melanoma or renal cell cancer using high-dose bolus interleukin 2. *JAMA* 1994;271:907–13.
8 Rosenberg SA. Il-2: the first effective immunotherapy for human cancer. *J Immunol* 2014;192:5451–8.
9 Cesana GC, DeRaffele G, Cohen S, *et al*. Characterization of CD4+CD25+ regulatory T cells in patients treated with high-dose interleukin-2 for metastatic melanoma or renal cell carcinoma. *J Clin Oncol* 2006;24:1169–77.
10 Dutcher JP, Schwartzentruber DJ, Kaufman HL, *et al*. High dose interleukin-2 (Aldesleukin) - expert consensus on best management practices-2014. *J Immunother Cancer* 2014;2:26.
11 Li Q, Yan Y, Liu J, *et al*. Toll-Like receptor 7 activation enhances CD8+ T cell effector functions by promoting cellular glycolysis. *Front Immunol* 2019;10:1–14.
12 Crittenden MR, Zebertavage L, Kramer G, *et al*. Tumor cure by radiation therapy and checkpoint inhibitors depends on pre-existing immunity. *Sci Rep* 2018;8:1–15.
13 Apetoh L, Ghiringhelli F, Tesniere A, *et al*. Toll-like receptor 4-dependent contribution of the immune system to anticancer chemotherapy and radiotherapy. *Nat Med* 2007;13:1050–9.
14 Lugade AA, Moran JP, Gerber SA, *et al*. Local radiation therapy of B16 melanoma tumors increases the generation of tumor antigen-specific effector cells that traffic to the tumor. *J Immunol* 2005;174:7516–23.
15 Connolly KA, Belt BA, Figueroa NM, *et al*. Increasing the efficacy of radiotherapy by modulating the CCR2/CCR5 chemokine axes. *Oncotarget* 2016;7:86522–35.
16 Walker JM, Rolig AS, Charych DH, *et al*. NKTR-214 immunotherapy synergizes with radiotherapy to stimulate systemic $CD8^+$ T cell responses capable of curing multi-focal cancer. *J Immunother Cancer* 2020;8:e000464–13.
17 Kadowaki N, Ho S, Antonenko S, *et al*. Subsets of human dendritic cell precursors express different toll-like receptors and respond to different microbial antigens. *J Exp Med* 2001;194:863–70.
18 Lee J, Chuang T-H, Redecke V, *et al*. Molecular basis for the immunostimulatory activity of guanine nucleoside analogs: activation of Toll-like receptor 7. *Proc Natl Acad Sci U S A* 2003;100:6646–51.
19 Li K, Qu S, Chen X, *et al*. Promising targets for cancer immunotherapy: TLRs, RLRs, and STING-mediated innate immune pathways. *Int J Mol Sci* 2017;18. doi:10.3390/ijms18020404. [Epub ahead of print: 14 Feb 2017].
20 Pieper AA, Rakhmilevich AL, Spiegelman DV, *et al*. Combination of radiation therapy, bempegaldesleukin, and checkpoint blockade eradicates advanced solid tumors and metastases in mice. *J Immunother Cancer* 2021;9:e002715.
21 Formenti SC, Demaria S. Systemic effects of local radiotherapy. *Lancet Oncol* 2009;10:718–26.
22 Moran AE, Polesso F, Weinberg AD. Cd8 T cells in situ function of high-affinity tumor-infiltrating immunotherapy expands and maintains the immunotherapy expands and maintains the function of high-affinity tumor-infiltrating CD8 T cells in situ. *Roswell Park Cancer Inst J Immunol* 2016;197:2509–21.
23 Zhou Z, Yu X, Zhang J, *et al*. Tlr7/8 agonists promote NK-DC cross-talk to enhance NK cell anti-tumor effects in hepatocellular carcinoma. *Cancer Lett* 2015;369:298–306.
24 Kim T-S, Shin E-C. The activation of bystander $CD8^+$ T cells and their roles in viral infection. *Exp Mol Med* 2019;51:1–9.
25 Burnette BC, Liang H, Lee Y, *et al*. The efficacy of radiotherapy relies upon induction of type I interferon-dependent innate and adaptive immunity. *Cancer Res* 2011;71:2488–96.
26 Simmons DP, Wearsch PA, Canaday DH, *et al*. Type I IFN drives a distinctive dendritic cell maturation phenotype that allows continued class II MHC synthesis and antigen processing. *J Immunol* 2012;188:3116–26.
27 Blair TC, Bambina S, Alice AF, *et al*. Dendritic cell maturation defines immunological responsiveness of tumors to radiation therapy. *J Immunol* 2020;204:3416–24.
28 DeVita VT, Chu E. A history of cancer chemotherapy. *Cancer Res* 2008;68:8643–53.
29 Bentebibel S-E, Hurwitz ME, Bernatchez C, *et al*. A first-in-human study and biomarker analysis of NKTR-214, a novel IL2Rβγ-biased cytokine, in patients with advanced or metastatic solid tumors. *Cancer Discov* 2019;9:711–21.
30 Diab A, Tannir NM, Bentebibel S-E, *et al*. Bempegaldesleukin (NKTR-214) plus nivolumab in patients with advanced solid tumors: phase I dose-escalation study of safety, efficacy, and immune activation (PIVOT-02). *Cancer Discov* 2020;10:1158–73.
31 Sia J, Szmyd R, Hau E, *et al*. Molecular mechanisms of radiation-induced cancer cell death: a primer. *Front. Cell Dev. Biol.* 2020;8:1–8.
32 Dajon M, Iribarren K, Cremer I. Toll-like receptor stimulation in cancer: a pro- and anti-tumor double-edged sword. *Immunobiology* 2017;222:89–100.
33 Stary G, Bangert C, Tauber M, *et al*. Tumoricidal activity of TLR7/8-activated inflammatory dendritic cells. *J Exp Med* 2007;204:1441–51.
34 Raeber ME, Rosalia RA, Schmid D, *et al*. Interleukin-2 signals converge in a lymphoid-dendritic cell pathway that promotes anticancer immunity. *Sci Transl Med* 2020;12. doi:10.1126/scitranslmed.aba5464. [Epub ahead of print: 16 09 2020].
35 Schölch S, Rauber C, Tietz A, *et al*. Radiotherapy combined with TLR7/8 activation induces strong immune responses against gastrointestinal tumors. *Oncotarget* 2015;6:4663–76.
36 Lorenzi S, Mattei F, Sistigu A, *et al*. Type I IFNs control antigen retention and survival of CD8α(+) dendritic cells after uptake of tumor apoptotic cells leading to cross-priming. *J Immunol* 2011;186:5142–50.
37 Pilones KA, Charpentier M, Garcia-Martinez E, *et al*. Radiotherapy cooperates with IL15 to induce antitumor immune responses. *Cancer Immunol Res* 2020;8:1054–63.
38 Dewan MZ, Galloway AE, Kawashima N, *et al*. Fractionated but not single-dose radiotherapy induces an immune-mediated abscopal effect when combined with anti-CTLA-4 antibody. *Clin Cancer Res* 2009;15:5379–88.
39 Monjazeb AM, Tietze JK, Grossenbacher SK, *et al*. Bystander activation and anti-tumor effects of CD8+ T cells following interleukin-2 based immunotherapy is independent of CD4+ T cell help. *PLoS One* 2014;9:e102709.
40 Chu T, Tyznik AJ, Roepke S, *et al*. Bystander-activated memory CD8 T cells control early pathogen load in an innate-like, NKG2D-dependent manner. *Cell Rep* 2013;3:701–8.
41 Duhen T, Duhen R, Montler R, *et al*. Co-expression of CD39 and CD103 identifies tumor-reactive CD8 T cells in human solid tumors. *Nat Commun* 2018;9:2724.